3D-U-SAM NETWORK FOR FEW-SHOT TOOTH SEGMENTATION IN CBCT IMAGES

Yifu ZHANG[1] *Zuozhu LIU*[2] *Yang FENG*[3] *Renjing XU*[1]

[1] The Hong Kong University of Science and Technology (Guangzhou), Guangzhou 511458, China

[2] Zhejiang University-University of Illinois at Urbana-Champaign InstituteZhejiang University, Haining 314400, China

[3] Angelalign Inc., Shanghai 200433, China

ABSTRACT

Accurate representation of tooth position is extremely important in treatment. 3D dental image segmentation is a widely used method, however labelled 3D dental datasets are a scarce resource, leading to the problem of small samples that this task faces in many cases. To this end, we address this problem with a pretrained SAM and propose a novel 3D-U-SAM network for 3D dental image segmentation. Specifically, in order to solve the problem of using 2D pre-trained weights on 3D datasets, we adopted a convolution approximation method; in order to retain more details, we designed skip connections to fuse features at all levels with reference to U-Net. The effectiveness of the proposed method is demonstrated in ablation experiments, comparison experiments, and sample size experiments.

***Index Terms*—** 3D Dental Image Segmentation, Deep learning, SAM, U-Net

1. INTRODUCTION

Thanks to current clinical research and rapid advances in computer-aided diagnosis (CAD) systems, digital dentistry has improved the accuracy of orthodontic diagnosis, treatment planning, and surgical guidelines[1]. Unfortunately, traditional dental X-rays provide a 2D single-plane view of these roots and cannot give the exact spatial orientation of these roots concerning adjacent structures[2]. Therefore, accurate segmentation[3] of 3D images of jaws and roots plays an important role in clinical decision-making. However, dental images have problems such as misalignment, shape heterogeneity, and noise interference[1]. Therefore some traditional 3D segmentation methods are not suitable for tooth segmentation [4]. Deep learning has the potential to solve the above problems but requires large-scale annotated datasets. Public datasets are currently not available [1], as manual annotation of half-jaws by experienced experts usually takes about 15 to 30 minutes [5], which is tedious and labor-intensive.

Recently, the Large AI Model (LAM) [6] has shown impressive performance on various downstream tasks. The recently developed segmentation any model SAM[7] is a basic model that has strong generalization capabilities and has great potential and feasibility for solving tooth segmentation problems[8].

However, it is very challenging to adapt the original SAM architecture designed for 2D natural images to 3D medical images. Modifying the overall structure of the network will make the pre-trained weights of SAM unavailable, and will increase the requirements for memory and computing power. Therefore, how to effectively adjust the pre-trained parameters on 2D images to capture 3D spatial information is worth exploring. We use SAM's few-shot learning and powerful generalization capabilities to solve the problem of tooth 3D segmentation itself and its small sample size. Because the traditional SAM cannot perform 3D segmentation tasks, we adapt it from 2D to 3D to complete this task. In addition, SAM is trained on natural images and cannot be directly applied to 3D dental medical images with blurred boundaries. To this end, we refer to U-Net[9] to extract deep features at various levels in the encoder part and fuse them to preserve details and propose a new architecture for 3D dental image segmentation, which we call 3D-U-SAM network. Surprisingly, the proposed method does not require too powerful computing power and can be run on a single RTX3090. The main contributions of this paper can be summarized as follows:

1. To the best of our knowledge, this work is the first attempt to apply SAM to 3D tooth segmentation to help solve the problem of 3D tooth segmentation in the case of small samples.

2. We modify the input-level image encoder to keep the original 2D pre-trained weights reusable and support 3D medical image input while reducing computation.

3. We refer to U-Net to elicit information between different layers of the image encoder, and then fuse them in the decoder. The goal is to fully exploit the abstraction features at all levels and preserve the details in dental images as much as possible.

The remainder of this paper is organized as follows. Section 2 details the proposed method and its background. Experi-

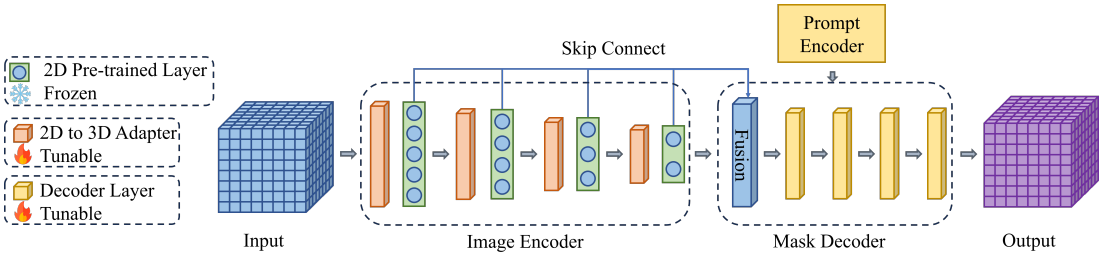

Fig. 1. The Overall Work.

mental results can be found in section 3. The conclusion is contained in section 4.

2. METHODS

2.1. Problem formulation

Given a tooth 3D segmentation dataset $\mathcal{D}_t = \{x_j, y_j\}_{j=1}^{n_t}$, where x_j is a tooth 3D image, y_j is a tooth 3D annotation (mask), and the data set has a total of n_t samples. Let the transformation of SAM be $\mathcal{SAM}_{2D}(\alpha)$, where α is the pre-trained parameter. At the same time given the transformation $\mathcal{USAM}_{3D}(\alpha, \theta)$ of 3D-U-SAM, The task considered is to use the training data set $\mathcal{D}_t$ to fine-tune the knowledge of tooth 3D segmentation $\mathcal{USAM}_{3D}(\alpha, \theta)$, learn the parameters $\widehat{\theta}$ and get the three-dimensional SAM transformation $\mathcal{USAM}_{3D}\left(\alpha, \widehat{\theta}\right)$ to improve the segmentation prediction results.

2.2. Overview of 3D-U-SAM

SAM consists of three parts: image encoder, hint encoder, and mask decoder. The image encoder utilizes the structure [10] of the visual transformer (ViT) to convert the raw image into an image embedding. The hint encoder encodes hints (points, boxes, etc.) into embedding representations, designing lightweight and learnable embedding sums by encoding frozen positions for each hint type. After an attention block, the feature map is upsampled and converted to a segmentation mask by MLP. However the above work is designed for 2D natural image segmentation and when it is applied directly to 3D images it will predict the 2D slices of the 3D image which will lose the information between each slice. To this end, we have made targeted adjustments, which can be found in section 2.3. In addition, due to the domain gap between natural images and dental medical images, such as natural images have more obvious contours, while medical images have the possibility of blurred boundaries, and the model also exhibits performance degradation when tested on medical images. We improve it concerning U-Net, which is detailed in Section 2.4. The structure of the overall work is shown in figure 1.

2.3. The 3D Encoded Feature Extractor

To allow the SAM model to directly learn 3D data, and inherit most of the model parameters pre-trained with 2D images and then fine-tuned, we did not follow the traditional method of slicing first and then merging [11]. This is because every dimension of a 3D dental medical image is equally important, and the spatial relationship between pixels is the same as in the two-dimensional case. Also, for this reason, a fully trained 2D spatial feature extraction network has the potential to extract 3D abstract features.

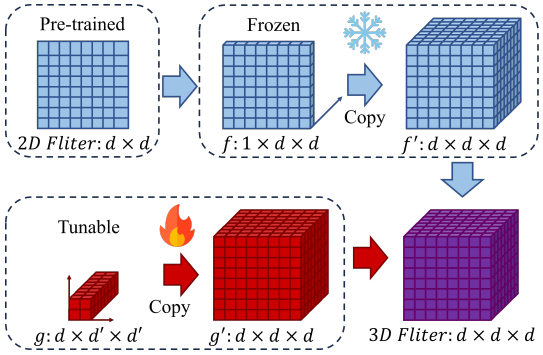

Fig. 2. 2D to 3D Adapter.

As shown in Fig.2, let the size of the 2D convolution F_{2D} in the original SAM be $d \times d$, we need to approximate it as a 3D convolution of $d \times d \times d$. Specifically, we initialize a tensor $1 \times d \times d$ with pre-trained 2D convolution kernel f weights and replicate d times in the first dimension. Expand it into a tensor f' of $d \times d \times d$. Then, randomly initialize a convolution kernel g of $d \times d' \times d'$, and expand it into a tensor g' of $d \times d \times d$. The convolution kernel size parameter d' can be selected according to requirements. Finally, a 3D convolution operation is performed on f' and g', and the parameters of f are kept unchanged during the training process. Finally, a network parameter is obtained as an output tensor F_{3D} of $d \times d \times d$.

$$F_{3D} = f' * g' \tag{1}$$

Using this method, the fully trained 2D convolution can be used to approximate the 3D convolution, and the number of

adjustable parameters from the original $104.06M$ can be reduced to $15.21M$ to save computing power. Because only g is needed to make our method work, there is no need to retrain all parameters.

2.4. Information Fusion Decoder

Directly using the structure from the original SAM iterative segmentation mode may cause some problems. First, we replace all 2D convolutions with 3D convolutions to directly generate 3D masks. Second, the original decoder structure is designed for [12] for natural images where the object size is usually large and the boundaries are clear. Objects in medical images are usually small and ill-defined, which require details and higher resolution for better distinction. U-Net is widely used in medical image segmentation because it has multiple levels of skip connections, and it is generally believed that it can preserve as much detail as possible in segmentation tasks. Therefore, we refer to U-Net to upsample the $N_{encoder}$ outputs in the middle of the encoder to the original resolution and fuse them. To save computing resources, we refer to our previous work [13, 14] to fuse them by summation, and then generate mask feature maps in a lightweight decoder. Specifically, the first convolutional layer of the decoder is taken out separately to form a feature fusion layer. The fusion layer can be regarded as the transformation $G_1(\cdot) = W_1(\cdot)$, where W_1 is the parameter that needs to be learned. We sum the abstract features $\mathcal{X}_i \left|_{i=1}^{N}\right.$ from all encoder convolutional layers in front of it. Then a new feature map $\mathcal{X}^1$ is obtained through the fusion layer.

$$\mathcal{X}^1 = G_1\left(\sum_{i=1}^{N}\mathcal{X}_i\right) = W_1\left(\sum_{i=1}^{N}\mathcal{X}_i\right) \tag{2}$$

Then enter the other layers of the decoder $G_2(\cdot)\cdots G_{N\,decoder}(\cdot)$, and output the predicted segmentation results. The parameters $W_k \left|_{k=1}^{N_{decoder}}\right.$ of each layer of the decoder will be updated by the labeled target domain data. Denote all parameters as $\theta_{decoder}$:

$$\theta_{decoder} = \{W_1; W_2 \cdots W_{N_{decoder}}\} \tag{3}$$

We introduce an overall scheme to adapt SAM for medical image segmentation. The focus of image encoder adaptation is how to effectively use pre-trained parameters to extract 3D spatial features, and it is also conducive to the model to better meet the needs of specific fields. Combining them, 3D-U-SAM becomes a potentially powerful volumetric medical image segmentation tool.

3. EXPERIMENTS

3.1. Dataset description

In this paper, the dataset comes from CTooth+[15], which fully preserves the three-dimensional features of teeth, and the number of data samples exceeds 30k slices, far exceeding the existing 2D dental datasets. The dataset consists of 5504 annotated CBCT images of 22 patients and 25876 unlabeled images of 146 patients. We selected 10 annotated data as the training set, 10 as the validation set, and 10 as the testing set. Because our purpose is to verify the performance of the proposed method under small sample conditions, and a larger verification set and test set can more accurately reflect the performance of the proposed method, we did not follow the conventional $8:1:1$ or $6:2:2$ divides the data set.

3.2. Experiment settings

In addition to the application, the innovation of this paper also has design rules to make SAM run on 3D dental medical image tasks while retaining the original SAM pre-training parameters. The U-Net idea is adopted to integrate information at all levels. Therefore, in terms of ablation experiments, this paper needs to verify the effectiveness of convolution approximation and the effectiveness of information fusion. Besides, we also compare some popular other 3D image segmentation methods. For example 3D-Unet[16], Two-Stage framework based on Mesh Deep Learning[17] and Self-Supervised Learning framework[1].

The experimental environment is NVIDIA GeForce RTX 3090 GPU, 12^{th} Gen Intel® Core™ i9-12900K Processor, with 32G memory computer, and the development tools are Python 3.9 and Pytorch 1.10.2. The random seed is set to 0 to avoid chance during model training. Due to the limitation of computing resources, the amount of data in each batch in the cutting task is small, so the method of group normalization is adopted to normalize the Similar to our previous work [13], IOU and F_β were selected as indicators. We chose to take different β values. They are F_1 score ($Dice\ score$), F_2 score and $F_{0.5}$ score respectively. The F_2 score indicates that the recall weight is higher than the precision. The $F_{0.5}$ score indicates that the precision weight is higher than the recall rate.

$$\begin{aligned} F_\beta &= \left(1+\beta^2\right) \times \frac{Precision \times Recall}{\left(\beta^2 \times Precision\right) + Recall} \\ &= \frac{\left(1+\beta^2\right) \times TP}{\left(1+\beta^2\right) \times TP + \beta^2 \times FN + FP} \end{aligned} \tag{4}$$

3.3. Results and analysis

3.3.1. Ablation experiment

We test the proposed method against two ablation experiments in Section 3.2, Among them, 3DUS represents the proposed method 3D-U-SAM, 3DUS* represents the deletion of convolution approximation, and the experiment is performed by slice; 3DUS** represents the fusion of deletion information, and the experimental results are shown in

the table 1. It can be seen that 3DUS achieves the best performance. 3DUS* works the worst because it processes 3D image slices the same way as 2D images, ignoring the relationship between slices. The effect of 3DUS** is in between them, and even some results are close to 3DUS, and the details of our removal of skip connection loss negatively affect the performance less than 3DUS*.

Table 1. Ablation Experiment Results

Methods	$F_1(Dice)$	IOU	F_2	$F_{0.5}$
3DUS	91.04%	86.72%	93.05%	89.73%
3DUS*	74.89%	79.54%	82.19%	73.24%
3DUS**	81.51%	84.95%	78.29%	88.56%

3.3.2. Comparative Experiment

We also tested the 3D-Unet (represented by 3DU), Two-Stage framework based on Mesh Deep Learning (represented by TSMDL), and Self-Supervised Learning framework (represented by STSNet) mentioned in the 3.2 section) performance as a comparison, the experimental results are shown in the table 2. It can be seen that F_1 is 2.92% higher than the second place. IOU is 2.88% higher than the second place. F_2 is 12.16% higher than the second place. $F_{0.5}$ is 1.28% lower than the first place. It can be seen that our method achieves the best performance in both F_1 and IOU. F_2 is much higher than other methods, but $F_{0.5}$ is slightly behind STSNet, so we believe that the proposed method performs better in terms of recall than precision. Since $F_{0.5}$ is slightly behind other methods, and F_2 is much higher than other methods, it can be considered that the proposed method 3D-U-SAM achieves the best results.

Table 2. Compare Experiment Results

Methods	$F_1(Dice)$	IOU	F_2	$F_{0.5}$
3DU[16](FGCS,2020)	82.60%	76.45%	80.89%	79.43%
TSMDL[17](TMI,2022)	85.57%	73.11%	71.95%	88.40%
STSNet[1](TMI,2022)	88.12%	83.84%	80.27%	**91.01**%
3DUS	**91.04**%	**86.72**%	**93.05**%	89.73%

3.3.3. Sample Size Experiment

In order to verify the performance of our method in the case of small samples, we tested the performance under different sample sizes. It can be seen from 3 that when the sample size is 5, the four indicators are far lower than when the sample size is 10. When the sample size is 20, the differences between the four indicators are within 2%. Even when the sample size is 10, F_2 performs better than when the sample size is 20, which may be caused by the randomness of the experiment. Based on the above experimental results, we believe that the sample size of 5 is small and performs poorly. The effect is better when the sample size is 10 and 20, and their difference is limited. The results show that our model can achieve competitive results with only 10 samples.

Table 3. Sample Size Experiment Results

Sample Size	$F_1(Dice)$	IOU	F_2	$F_{0.5}$
5	79.99%	78.64%	80.03%	81.10%
10	91.04%	86.72%	**93.05**%	89.73%
20	**92.00**%	**88.09**%	92.96%	**91.45**%

The ablation experiment can prove that the idea of using the convolution approximation method in SAM to turn it into 3D and retain the details with a skip connection structure is feasible in the face of small sample dental 3D image segmentation. Comparative experiments show that our method is a competitive solution and contributes to the implementation of SAM-based methods in 3D dental image analysis. The results given from various sample sizes show that our model can achieve competitive results with only 10 samples when training.

4. CONCLUSION

A novel 3D-U-SAM network for 3D dental image segmentation is proposed. Specifically, by designing a 2D convolution to approximate a 3D convolution strategy, the amount of computation is reduced while ensuring that the original SAM pre-trained parameters are available. By designing a skip connection strategy, deep features at various levels are elicited in the encoder part and fused to preserve details. Three experimental results confirm the learning ability of the 3D-U-SAM network in small sample situations.

5. REFERENCES

[1] Zuozhu Liu, Xiaoxuan He, Hualiang Wang, Huimin Xiong, Yan Zhang, Gaoang Wang, Jin Hao, Yang Feng, Fudong Zhu, and Haoji Hu, "Hierarchical self-supervised learning for 3d tooth segmentation in intra-oral mesh scans," *IEEE Transactions on Medical Imaging*, vol. 42, no. 2, pp. 467–480, 2022.

[2] Dong Xu Ji, Sim Heng Ong, and Kelvin Weng Chiong Foong, "A level-set based approach for anterior teeth segmentation in cone beam computed tomography images," *Computers in biology and medicine*, vol. 50, pp. 116–128, 2014.

[3] Weiwei Cui, Yaqi Wang, Qianni Zhang, Huiyu Zhou, Dan Song, Xingyong Zuo, Gangyong Jia, and Liaoyuan Zeng, "Ctooth: a fully annotated 3d dataset and benchmark for tooth volume segmentation on cone beam computed tomography images," in *International Confer-*

ence on Intelligent Robotics and Applications. Springer, 2022, pp. 191–200.

[4] Shizhan Gong, Yuan Zhong, Wenao Ma, Jinpeng Li, Zhao Wang, Jingyang Zhang, Pheng-Ann Heng, and Qi Dou, "3dsam-adapter: Holistic adaptation of sam from 2d to 3d for promptable medical image segmentation," *arXiv preprint arXiv:2306.13465*, 2023.

[5] J Hao, W Liao, YL Zhang, J Peng, Z Zhao, Z Chen, BW Zhou, Y Feng, B Fang, ZZ Liu, et al., "Toward clinically applicable 3-dimensional tooth segmentation via deep learning," *Journal of dental research*, vol. 101, no. 3, pp. 304–311, 2022.

[6] R OpenAI, "Gpt-4 technical report," *arXiv*, pp. 2303–08774, 2023.

[7] Alexander Kirillov, Eric Mintun, Nikhila Ravi, Hanzi Mao, Chloe Rolland, Laura Gustafson, Tete Xiao, Spencer Whitehead, Alexander C Berg, Wan-Yen Lo, et al., "Segment anything," *arXiv preprint arXiv:2304.02643*, 2023.

[8] Maciej A Mazurowski, Haoyu Dong, Hanxue Gu, Jichen Yang, Nicholas Konz, and Yixin Zhang, "Segment anything model for medical image analysis: an experimental study," *Medical Image Analysis*, vol. 89, pp. 102918, 2023.

[9] Olaf Ronneberger, Philipp Fischer, and Thomas Brox, "U-net: Convolutional networks for biomedical image segmentation," in *Medical Image Computing and Computer-Assisted Intervention–MICCAI 2015: 18th International Conference, Munich, Germany, October 5-9, 2015, Proceedings, Part III 18*. Springer, 2015, pp. 234–241.

[10] Alexey Dosovitskiy, Lucas Beyer, Alexander Kolesnikov, Dirk Weissenborn, Xiaohua Zhai, Thomas Unterthiner, Mostafa Dehghani, Matthias Minderer, Georg Heigold, Sylvain Gelly, et al., "An image is worth 16x16 words: Transformers for image recognition at scale," *arXiv preprint arXiv:2010.11929*, 2020.

[11] Taojiannan Yang, Yi Zhu, Yusheng Xie, Aston Zhang, Chen Chen, and Mu Li, "Aim: Adapting image models for efficient video action recognition," *arXiv preprint arXiv:2302.03024*, 2023.

[12] Yuhao Huang, Xin Yang, Lian Liu, Han Zhou, Ao Chang, Xinrui Zhou, Rusi Chen, Junxuan Yu, Jiongquan Chen, Chaoyu Chen, et al., "Segment anything model for medical images?," *arXiv preprint arXiv:2304.14660*, 2023.

[13] Yifu Zhang, Hongru Li, Tao Yang, Rui Tao, Zhengyuan Liu, Shimeng Shi, Jiansong Zhang, Ning Ma, Wujin Feng, Zhanhu Zhang, and Xinyu Zhang, "Multi-source adversarial transfer learning for ultrasound image segmentation with limited similarity," *Applied Soft Computing*, vol. 146, pp. 110675, 2023.

[14] Yifu Zhang, Hongru Li, Shimeng Shi, Youqi Li, and Jiansong Zhang, "Multi-source adversarial transfer learning based on similar source domains with local features," *arXiv preprint arXiv:2305.19067*, 2023.

[15] Weiwei Cui, Yaqi Wang, Yilong Li, Dan Song, Xingyong Zuo, Jiaojiao Wang, Yifan Zhang, Huiyu Zhou, Bung san Chong, Liaoyuan Zeng, et al., "Ctooth+: A large-scale dental cone beam computed tomography dataset and benchmark for tooth volume segmentation," in *MICCAI Workshop on Data Augmentation, Labelling, and Imperfections*. Springer, 2022, pp. 64–73.

[16] Saqib Qamar, Hai Jin, Ran Zheng, Parvez Ahmad, and Mohd Usama, "A variant form of 3d-unet for infant brain segmentation," *Future Generation Computer Systems*, vol. 108, pp. 613–623, 2020.

[17] Tai-Hsien Wu, Chunfeng Lian, Sanghee Lee, Matthew Pastewait, Christian Piers, Jie Liu, Fan Wang, Li Wang, Chiung-Ying Chiu, Wenchi Wang, et al., "Two-stage mesh deep learning for automated tooth segmentation and landmark localization on 3d intraoral scans," *IEEE Transactions on Medical Imaging*, vol. 41, no. 11, pp. 3158–3166, 2022.